SOME RESULTS IN MODEL BASED TRANSVERSE CRACK IDENTIFICATION IN ROTOR SYSTEMS

Nicolò Bachschmid[(1)]
Paolo Pennacchi[(1)]
Sylvie Audebert[(2)]
(1) Dipartimento di Meccanica, Politecnico di Milano,
P.zza Leonardo da Vinci, 32 - I-20133 Milano, Italy
e-mail nicolo.bachschmid@polimi.it, paolo.pennacchi@mecc.polimi.it
(2) Division Recherche et Développement, Dép. Acoustique et Mécanique Vibratoire
EDF - Electricité de France 1, avenue du Général de Gaulle - 92141 Clamart CEDEX,
France, e-mail sylvie.audebert@edf.fr

Abstract

This paper presents some experimental results obtained on the EUROPE (Ensamble Utilisant un ROtor Pour Essais) test rig, which was expressly designed by EDF (Electricité de France) for investigating the dynamical behavior of cracked rotors. The results are used for validating a model based transverse crack identification method, which was developed during an European community funded research project called MODIAROT (MOdel based DIAgnosis of ROTor systems in power plants). The excellent accuracy obtained in identifying position and depth a crack proves the effectiveness and reliability of the proposed method.

Keywords: Identification, Crack, Rotordynamics.

1. INTRODUCTION

Propagating transverse cracks have been discovered in the last 20 years (Allianz, 1987) in several rotors of steam turbines or generators of European power plants. Fortunately, as far as the authors know, they have been detected before the crack had propagated to a critical depth, that means before the occurrence of a catastrophic failure.

The importance of early detection of cracks, possibly by means of an automatic diagnostic methodology that uses the informations furnished by standard monitoring systems, which generally analyze the vibrations measured in correspondence of the bearings only, appears obvious from these considerations.

The dynamical behavior of rotors with transverse crack has been studied by many authors (an extensive survey is given in Dimarogonas, 1996) and therefore the symptoms of a cracked rotor are well known: a change in 1x rev., 2x rev. and 3x rev vibration vector is suspect. A change in vibration vector means not just an increase or a decrease in amplitude, but also a change in phase only with constant amplitude. However, 1x rev. components can be caused by many other faults (e.g. unbalance, bow, coupling misalignments) and 2x rev. components can be due also to polar stiffness asymmetries (in generators), to surface geometry errors

(journal ovalization) and to non-linear effects in oil film bearings. These two last causes can also generate 3x rev. components.

It is then extremely important to have a reference situation, stored by the monitoring system, in which the behavior of the rotor system without faults and in similar operating conditions is analyzed. The reference situation would be better represented by run-down transient which furnishes much more informations about its dynamical behavior, rather than by a steady state condition at normal operating speed. By comparing then the actual behavior during a run-down transient with the reference behavior, the change in vibrations can be evaluated and by means of one of the automatic diagnostic procedures based on fault-symptom matrices or on decision trees approach, the type of the most probable impending fault can be identified.

Once the type of fault has been identified in a shaft line, also its most probable position and its severity (f.i. in the case of a crack, its depth) should be identified. This is then possible by means of the least square approach in the frequency domain, which is described in the following paragraph.

2. MODEL BASED IDENTIFICATION

As described in (Bachschmid et al. 2000), assuming a finite beam element model for the rotor, the effect of a crack on the statical and dynamical behavior of the rotor can be simulated in the frequency domain, by applying to the rotor different sets of equivalent forces, one set for each one of the three harmonic components in correspondence of the cracked beam element. The problem of the identification of the position of the crack is then reduced to an external force identification procedure, described in (Bachschmid et al. 1999). The final equations are recalled here below.

The difference, between the measured vibration of rotor system that has a fault and the reference case, represents the vibrational behavior due to the fault. These vibrations are then used in the identification procedure. By applying the harmonic balance criteria in the frequency domain, the differences δ_n, between the vibrations, which are calculated by means of suitable models of the system and of the fault, and measured vibrations X_{Bmn} can be defined for each harmonic component as:

$$\delta_n = \alpha_{B_n} \cdot F_{f_n} - X_{Bm_n} \tag{1}$$

where α_{Bn} is the partitioned inverse of the system dynamical stiffness matrix and F_{fn} is the n-th component of the fault force vector. Eq (1) can be written for each one of the different rotating speeds which are taken into consideration for the identification. Since the unknown force vector is composed by few forces applied to 2 nodes only of the f.e. model, the unknowns are much less than the number of the equations (1) and a least square approach can be used.

A relative residual may be defined by the root of the ratio of the squared δ_n, divided by the sum of the squared measured vibration amplitudes X_{Bmn}:

$$\delta_{r\,n} = \left(\frac{\left[\alpha_{B_n} \cdot F_{f_n} - X_{Bm\,n}\right]^T \left[\alpha_{B_n} \cdot F_{f_n} - X_{Bm_n}\right]}{X_{Bm_n}{}^T X_{Bm_n}} \right)^{1/2} \tag{2}$$

By means of the hypothesis of localization of the fault, the residual is calculated for each possible node of application of the defect. The set of equivalent forces in the case of a crack can be reduced to a couple of opposite and equal moments which have 1x rev., 2x rev. and 3x rev. components.

Where the residual reaches its minimum, there is the most probable position of the crack. It is worth noting that the 1x rev. vibration components are due both to the breathing mechanism of the crack and to the local bow which generally has developed during the crack propagation. Therefore, when no other sources of bow are present, the 1x rev. component is useful for the localization of the crack, but not for the identification of its depth.

The 3x rev. component is rather small and generally masked by some noise. Often this component can be recognized only when approaching the resonant condition at a rotating speed equal to 1/3 the rotor's critical speed.

The 2x rev. component is therefore the most suitable symptom for detecting position and depth of the crack; the highest values are obviously reached during a run-down transient when approaching the resonant condition at 1/2 critical speed.

3. CRACK DEPTH IDENTIFICATION

The following procedure has been implemented for the identification of the crack depth. The L.S. identification procedure, described in the previous paragraph, identifies the crack position in a particular element of the rotor, whose length is known from the 2D f.e.m. and equal to l. The *"equivalent"* moment components M_n (1x, 2x and 3x rev. components) are applied to this element. These equivalent bending moment components M_1, M_2 and M_3 have been calculated from the corresponding 1x, 2x and 3x rev. measured vibrational behavior.

Then the statical bending moment M in correspondence of the same element, due to the weight and to bearing alignment conditions, is calculated from model data.

The ratios of the nx rev. equivalent bending moment M_n to the statical bending moment M are all dependent on the relative crack depth p only. This is represented in Figure 1 for the 1x, 2x and 3x rev. component and expressed by the relationship in eq. (3).

$$\frac{M_n}{M} = f(p) \tag{3}$$

In the same figure also the curve M_2/M for an always open crack (a slot or notch) is shown: in this case the 2x rev. component only is present and 1x and 3x rev. component are absent. Eq. (3) can then be used for determining the crack depth. But, as shown in (Bachschmid et al. 2000), the length l_c of the *"equivalent"*, reduced stiffness, beam element that simulates the behavior of the cracked beam, is also depending on the relative crack depth p:

$$\frac{l_c}{D} = g(p) \tag{4}$$

The function $g(p)$ is represented in Figure 2. Now we have the equivalent bending moments M_n which are applied to an element with a wrong length: l instead of l_c. It is worth noting that the nx rev. measured displacements are due to the relative rotation of the cracked element extremity nodes, which is proportional to the product $M_n \cdot l$ of the identified nx rev. bending moment component applied to one element of the f.e. model of the rotor, multiplied by its length.

The equivalent bending moment component M'_n, applied to an equivalent cracked beam element of length l_c, can therefore be calculated as:

$$M'_n \cdot l_c = M_n \cdot l \tag{5}$$

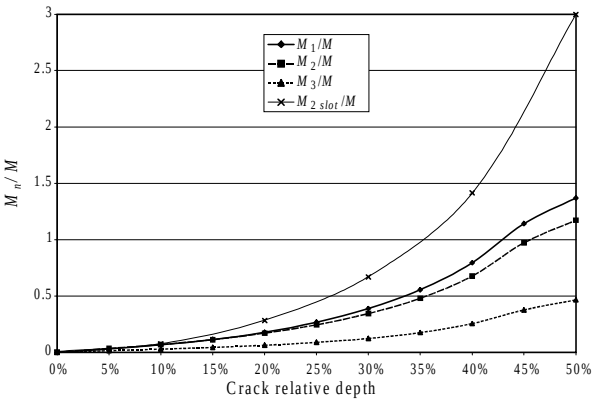

Figure 1. Bending moments ratio on the equivalent cracked beam, as a function of crack relative depth for the *n*x rev. component.

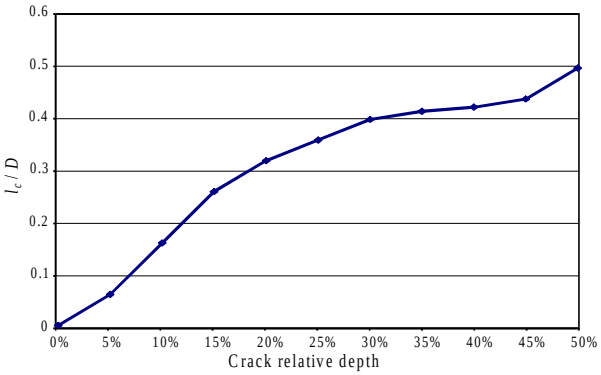

Figure 2. Relationship between the crack relative depth *p*, the diameter *D* and the length l_c of *"equivalent"* beam.

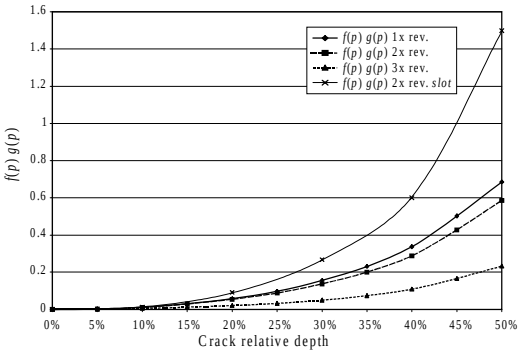

Figure 3. Function for the calculation of the crack depth.

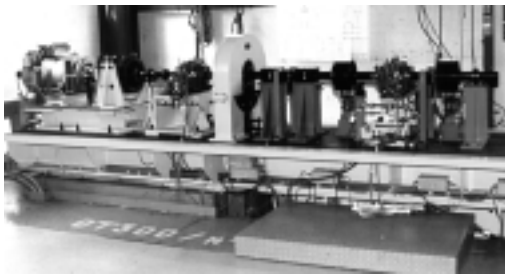

Figure 4. 2-bearing 1-composed shaft test rig of EDF-Electricité de France on rigid foundation.

By assuming that the statical bending moment *M* applied to the original element of length *l* does not change much along the element, the same *M* can be considered applied to the element with equivalent length l_c.

Recalling eq. (3) we can derive:

$$\frac{M_n'}{M} = \frac{M_n \cdot l}{M \cdot l_c} = f(p) \tag{6}$$

and using eq. (4) we get:

$$\frac{M_n \cdot l}{M \cdot D} = f(p) \cdot g(p) \tag{7}$$

Eq. (7), shown in Figure 3 for the *n*x rev. components, can then be used for determining, from the known left hand side, the relative depth of the crack.

4. EXPERIMENTAL RESULTS

4.1 EUROPE Test Rig Description

The EUROPE test rig, shown in Figure 4, is composed by a shaft divided in three parts supported by two equal three lobe oil film bearings. The nominal diameter of the shaft is 70 mm and the overall length is 3.15 m. The distance between the bearings is 1.88 m. The

total mass is 450 kg and the main inertia disk is of 250 kg. In this configuration the 1st critical speed is close to 1150 rpm. The supporting structure can be considered as rigid in the speed range 0÷1500 rpm. The proximity probes for the measurements of relative shaft-journal vibrations are close to the bearings, but not inside of them, as usually occurs in real machines.

Since the central part of the rotor can be disassembled, several types of crack can be generated. The crack, considered in this paper to validate the identification procedure, has been started from a notch and made grown up to a depth of 33 mm, which corresponds to a depth of 47% on a shaft of 70 mm of diameter.

The possibility of disassembling of the central part of the rotor has the main advantage to not dismount the entire rotor in order to create a crack. However this leads to some difficulties to have a valid reference case. In fact, by considering a run-down of the uncracked rotor and a run-down of a cracked one, small differences in alignment might be introduced when the central part is coupled to the other extremities. Moreover, the cracked part presents usually a permanent bow due to the fatigue solicitation used to generate the crack (see also §4.3).

4.2 Reference Situation

Even if the so-called *"reference situation"* cannot actually be considered as the true reference situation of the same rotor in this test rig, due to the reason previously expressed, nevertheless it has been used to calculate the vibration difference. The measured reference situation is reported in Figure 5 to Figure 10 for the 1x, 2x and 3x rev. components.

From the analysis of the 1x rev. component in Figure 5 and Figure 6, it is evident the critical speed at about 1150 rpm and that the rotor presents a bow which generates around 15 μm at very low speed in bearing 1.

As regards the 2x rev. component in Figure 7 and Figure 8 the second critical speed is rather evident at about 1/2 of the critical speed, but also a peak at about 1100 rpm that indicates a non linear effect of the oil film can be recognized. The relatively high value of the 2x rev. component in the second bearing (about 14 μm) at low speed, which remains the main component over all the speed range as is also shown by the phase trend, indicates a geometrical error of the shaft (journal ovalization) in the bearing. The phase difference of 180° between horizontal and vertical components is typical for ovalization errors. The 3x rev. component has very reduced amplitude in both bearings (about 1 μm and 4 μm respectively) and is mainly due to some noise, however a smaller peak at about 1/3 of the critical speed is recognizable.

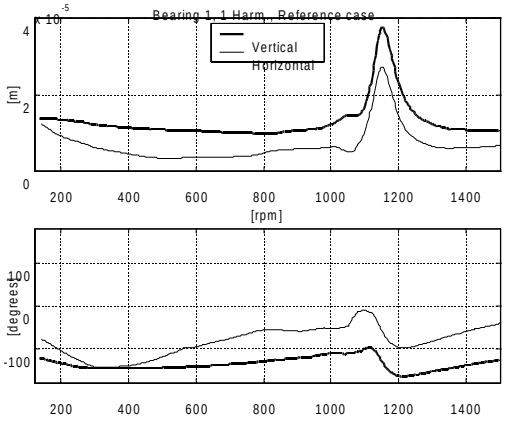

Figure 5. Reference case: 1x rev. vibration components for bearing 1.

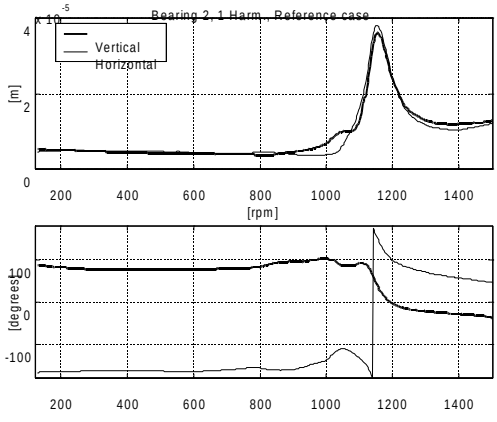

Figure 6. Reference case: 1x rev. vibration components for bearing 2.

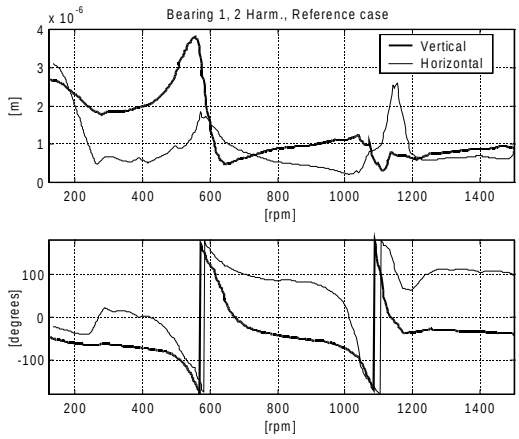

Figure 7. Reference case: 2x rev. vibration components for bearing 1.

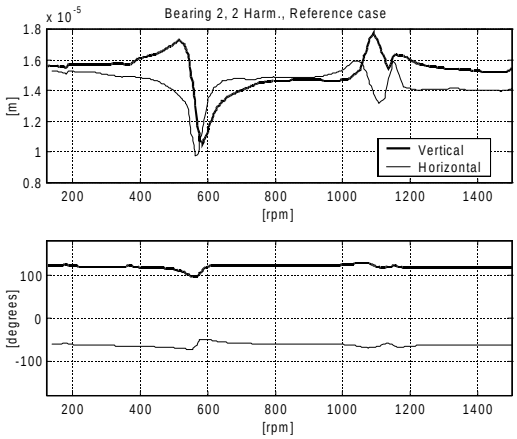

Figure 8. Reference case: 2x rev. vibration components for bearing 2.

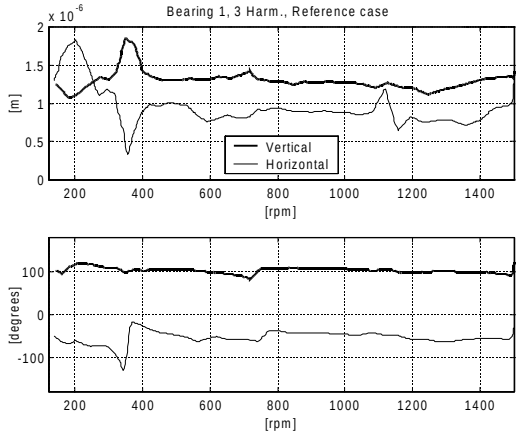

Figure 9. Reference case: 3x rev. vibration components for bearing 1.

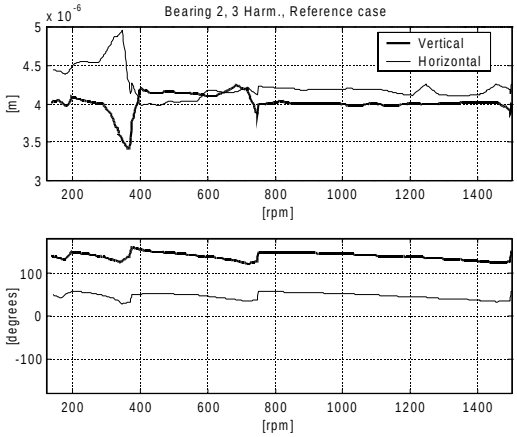

Figure 10. Reference case: 3x rev. vibration components for bearing 2.

4.3 Cracked Rotor

The experimental measures obtained with a crack of 47% depth of the diameter in the central section without subtracting the reference case are shown in Figure 11-Figure 16.

From the 1x rev. component (Figure 11 and Figure 12) it can be inferred that the rotor presents a permanent bow which is increased with respect to the reference rotor. As regards the 2x rev. component, the high amplitude (about 40 μm) of the peak at 1/2 critical speed is clearly due to the crack, which produces also a high resonance amplitude (about 10 μm) of the 3x rev. component at 1/3 critical speed.

By using the measured vibrations due to the crack and subtracting the reference case vibrations, an attempt to identify the position and the depth of the crack has been carried out. The results in Figure 17 show that the location of the crack is precisely identified by all the three harmonic components. Moreover, the 1x rev. component identifies the position with a particularly reduced value of the relative residual. This result has been obtained by processing the experimental data in the following way: first the unbalances on the disks were identified, and then the dynamical behavior due to the unbalances only has been subtracted from measured data in order to obtain the bow induced vibrations. This leads to a very good agreement between the experimental and the simulated behavior for the 1x rev. component as shown in Figure 18 and Figure 19, in which bow and unbalances have been superposed.

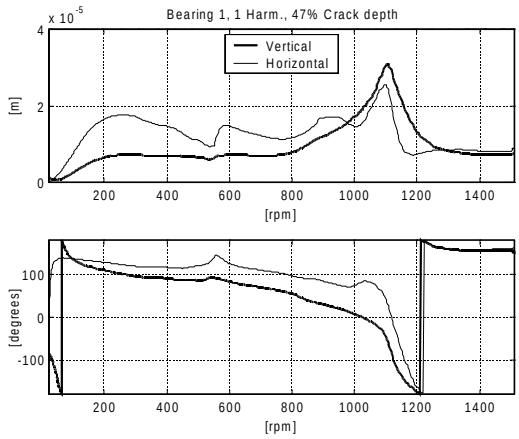

Figure 11. 47% crack: 1x rev. vibration components for bearing 1.

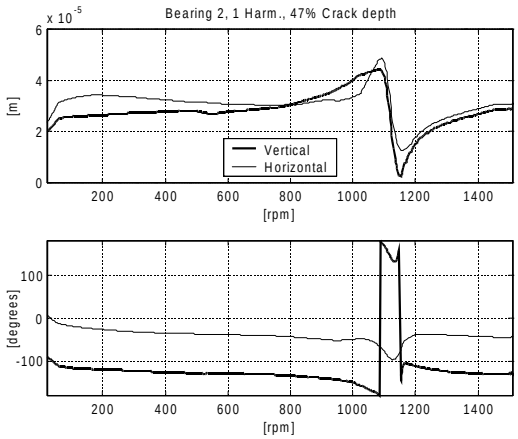

Figure 12. 47% crack: 1x rev. vibration components for bearing 2.

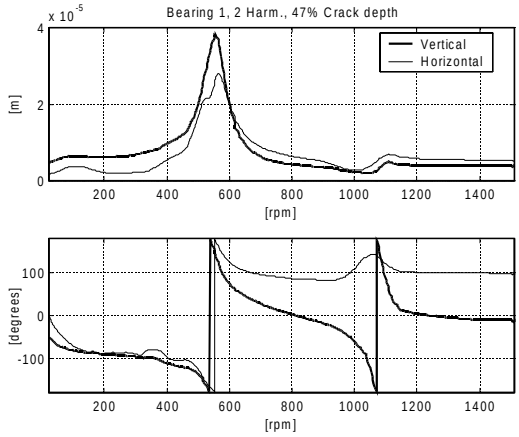

Figure 13. 47% crack: 2x rev. vibration components for bearing 1.

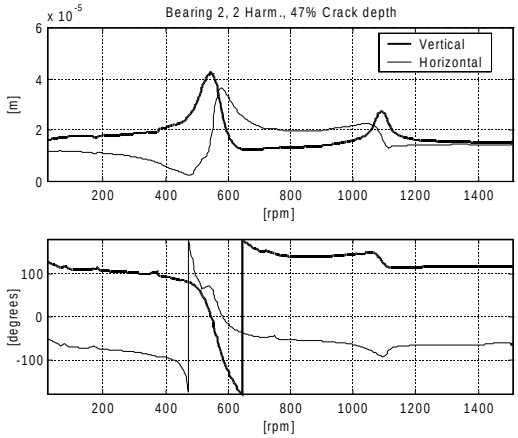

Figure 14. 47% crack: 2x rev. vibration components for bearing 2.

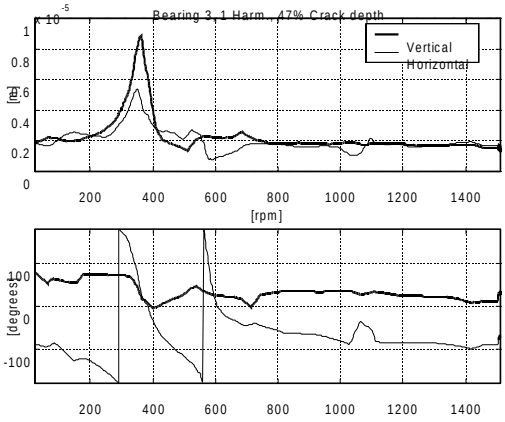

Figure 15. 47% crack: 3x rev. vibration components for bearing 1.

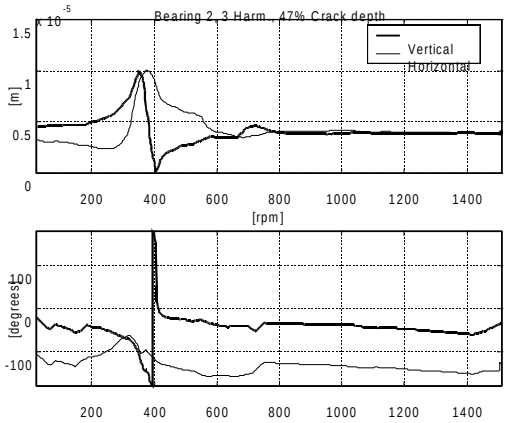

Figure 16. 47% crack: 3x rev. vibration components for bearing 2.

As regards the 2x rev. component, the relative residual can be considered as good, but the most remarkable result is the exact identification of the depth of the crack. Also the simulated behavior in Figure 20 and Figure 21 is good. As concerning the 3x rev. component, the relative residual is quite high, but this can be explained by considering that this component is normally masked by noise. However, the residual curve presents a well defined minimum in

correspondence of the crack even this is not so evident in Figure 17 due to the scale. For this component, the comparison is reported in Figure 22 and Figure 23.

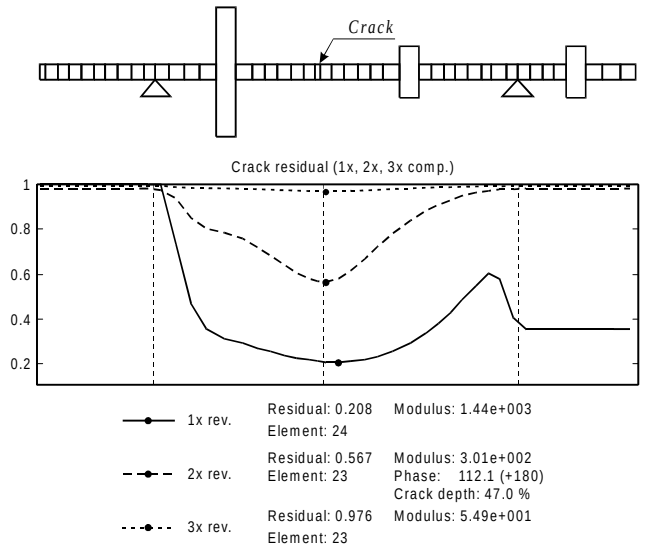

Figure 17. 47% cracked shaft. Relative residuals of the crack identification.

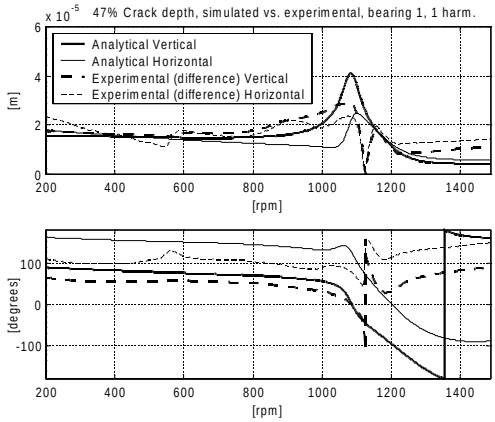

Figure 18. 47% crack: comparison between simulated and experimental (differences) 1x rev. vibration components for bearing 1.

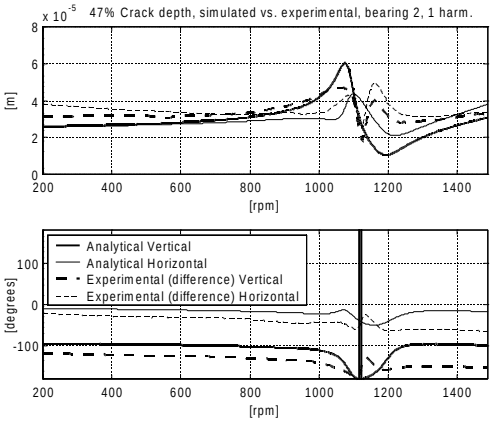

Figure 19. 47% crack: comparison between simulated and experimental (differences) 1x rev. vibration components for bearing 2.

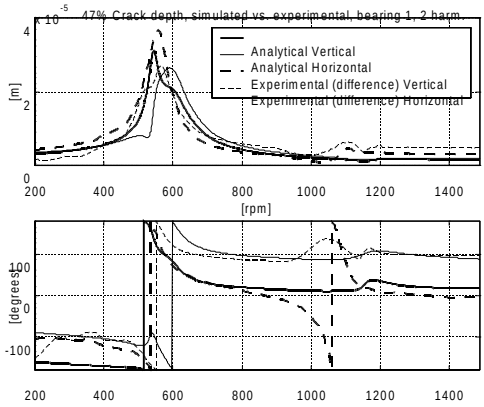

Figure 20. 47% crack: comparison between simulated and experimental (differences) 2x rev. vibration components for bearing 1.

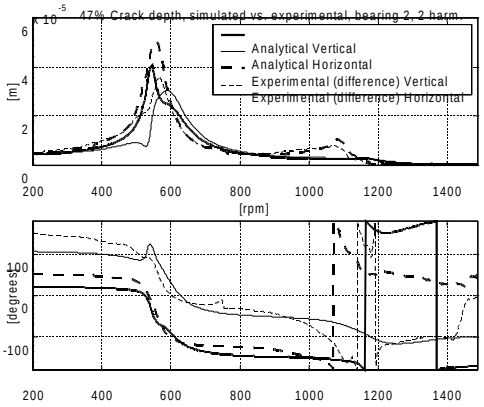

Figure 21. 47% crack: comparison between simulated and experimental (differences) 2x rev. vibration components for bearing 2.

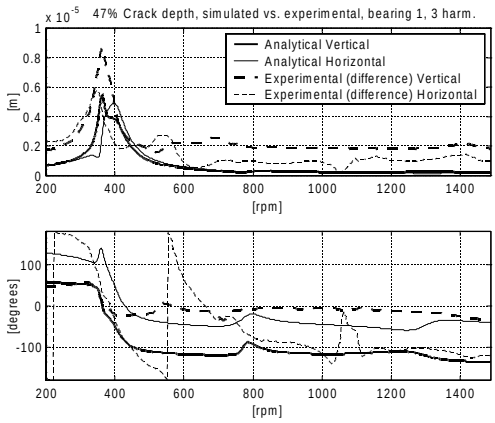

Figure 22. 47% crack: comparison between simulated and experimental (differences) 3x rev. vibration components for bearing 1.

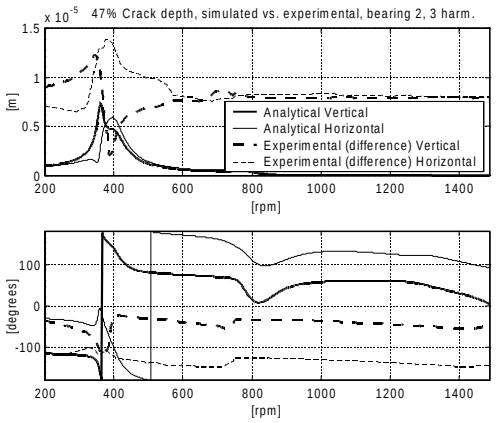

Figure 23. 47% crack: comparison between simulated and experimental (differences) 3x rev. vibration components for bearing 2.

5 CONCLUSIONS

These results, along with others referred to other test rigs or to other crack depths on the EUROPE test rig , validate the method proposed by the authors to identify the crack.

6 ACKNOWLEDGEMENTS

This work is partially funded by the MURST (Italian Ministry for the University and Scientific Research) Cofinanziamento "IDENTIFICAZIONE DI MALFUNZIONAMENTI IN SISTEMI MECCANICI" for the year 1999.

7 REFERENCES

Allianz, 1987, "ALLIANZ Berichte", nr. 24 Nov. 1987, ISSN 0569-0692.

Bachschmid N., Vania A., Tanzi E. and Pennacchi P., 1999, "Identification and Simulation of Faults in Rotor Systems: Experimental Results", *Proc. of EURO DINAME 99 - Dynamic Problems in Mechanics and Mechatronics*, Wissenschaftszentrum Schloß Reisenburg der Universität Ulm, 11-16 July 1999, Günzburg, Germany, pp. 3-11.

Bachschmid, N., Vania, A. and Audebert, S., 2000, "A Comparison of Different Methods for Transverse Crack Modelling in Rotor Systems", *Proc. of ISROMAC-8 Conference*, 26-30 March 2000, Honolulu, Hawaii, ISBN 0-9652469-9-X, pp. 1057-1064.

Dimarogonas, A.D., 1996, "Vibration of cracked structures. A state of the art review", *Engineering Fracture Mechanics*, 55, pp.831-857.